



## A neutron scattering study of the role of diffusion in the hydration of tricalcium silicate

S.A. FitzGerald<sup>a,\*</sup>, J.J. Thomas<sup>b</sup>, D.A. Neumann<sup>c</sup>, R.A. Livingston<sup>d</sup>

<sup>a</sup>*Oberlin College, Department of Physics, Oberlin, OH 44074, USA*

<sup>b</sup>*Northwestern University, Department of Civil Engineering, Evanston, IL 60208, USA*

<sup>c</sup>*NIST Center for Neutron Research, National Institute of Standards and Technology, Gaithersburg, MD 20899, USA*

<sup>d</sup>*Office of Infrastructure R&D, Federal Highway Administration, McLean, VA 22101, USA*

Received 8 August 2001; accepted 17 September 2001

### Abstract

Quasi-elastic neutron scattering was used to monitor the temperature-dependant hydration of tricalcium silicate and Portland cement. Results show that for some samples the degree of hydration is in fact higher at lower curing temperatures. To investigate this effect further, we performed a series of experiments in which samples are initially hydrated at one temperature and then the diffusion process limiting the long-term curing is monitored at a different temperature. The results confirm that the higher the initial curing temperature the more impervious are the product layers to later diffusion. In addition, it was found that the intrinsic activation energy for this diffusion process is much greater than the traditional values obtained using samples initially cured at different temperatures. © 2002 Elsevier Science Ltd. All rights reserved.

**Keywords:** Hydration; Kinetics; Neutron scattering; Diffusion;  $\text{Ca}_3\text{SiO}_5$

### 1. Introduction

Quasi-elastic neutron scattering (QENS) has recently emerged as a new technique for monitoring the hydration of cementitious materials [1–3]. This technique provides a direct measure of the conversion of free water to bound water throughout the curing process using measurements that can be made in-situ and without disturbing the sample. The resultant data expressed as a free water index (FWI) have been used to model the hydration kinetics during the three different curing stages known as induction, nucleation and growth, and finally diffusion limited behavior [1]. The QENS technique is particularly useful for monitoring the slower diffusion limited process because it does not suffer from any of the long time baseline problems associated with standard techniques such as isothermal calorimetry [4]. In this paper, we focus on this

diffusion limited process and in particular the effects of temperature on the kinetics and the chemical nature of the final product.

In Section 4, we demonstrate how QENS can be used to monitor the amount of free, constrained and bound water that is present in the sample. The data show that after an initial induction period, the reaction proceeds in a rapid growth process that is followed by a much slower diffusion limited process. Although the extracted diffusion constants, for this later stage, vary significantly for the different cements studied, there is relatively little temperature dependence to the diffusion constant within any given material. This is surprising, because intrinsic diffusion rates are expected to increase significantly with temperature.

In an earlier QENS paper [1], it was hypothesized that the lack of temperature dependence occurred because the hydration product formed at higher temperature is more impervious to diffusion, thus, offsetting the intrinsic increase in the rate of diffusion at higher temperature [5,6]. In the work reported here, this hypothesis was tested further and confirmed by performing a series of experiments in which the sample was cured at one temperature during the early nucleation and growth period and then

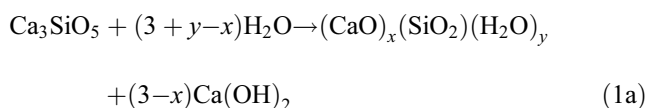
\* Corresponding author. University of Pittsburgh, Department of Chemistry, 234 Chevron Science Center, Pittsburgh, PA 15260, USA. Tel.: +1-412-624-8323; fax: +1-412-624-6003.

E-mail address: stephen.fitzgerald@oberlin.edu (S.A. FitzGerald).

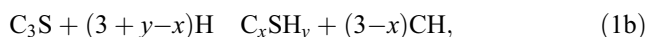
later diffusion-controlled kinetics were measured at a different temperature. In this way, the intrinsic activation energy could be extracted by studying the temperature dependence of the diffusion-controlled kinetics on nominally identical samples (i.e., samples that had been initially cured at the same temperature). As we will show, this intrinsic activation energy is considerably larger than the standard literature values quoted for samples initially cured at different temperatures.

## 2. Background

The reaction between tricalcium silicate ( $C_3S$ ) and water is the principal factor in the setting and hardening of Portland cement. This hydration process which proceeds in several steps can be summarized as [7] (Eq. (1a)):



which is written in cement notation as<sup>1</sup> (Eq. (1b)):



where  $x$  and  $y$  can change during the course of the reaction, particularly at very early times, and vary with position on a nanometer scale. Due to the complex chemical and physical nature of the C–S–H gel, it is difficult to arrive at a theoretically complete model of the kinetics of cement hydration. There are divergent opinions regarding the details of the hydration mechanisms, which are well summarized in various review articles [8,9]. A generally accepted overview of the process is that immediately after mixing there is a brief burst of dissolution and precipitation that is followed by the induction period lasting for a few hours (depending on temperature), after which the reaction rate rapidly increases. During the next period, the majority of the C–S–H gel-like material is formed through a solution process that follows nucleation and growth kinetics. When all of the available surface of the  $C_3S$  grains are coated with a sufficiently thick layer of C–S–H, the reaction becomes limited by the rate at which water can diffuse through the C–S–H to reach the unreacted  $C_3S$ .

## 3. Experimental technique

The hydration experiments were performed on Type I Portland cement (Lafarge Cement) and on two lots of  $C_3S$  powder obtained from different sources. The first lot was purchased from Construction Technology Laboratories

(CTL, Skokie, IL<sup>2</sup>), while the second was manufactured by calcining a 3:1 mixture of CaO and  $SiO_2$  powder at 1400 °C, and then grinding the resultant product in a mortar and pestle.<sup>3</sup> In all cases, the cement or  $C_3S$  was mixed with distilled water to produce a paste with a 0.4 water/cement ratio by mass. The paste was spread into a thin 0.5-mm layer on an aluminum cell, which was then sealed with an indium gasket. The sample was constrained to this thickness to mitigate the problem of multiple neutron scattering. The cell was lined with Teflon to prevent the sample from reacting with the aluminum sample holder. The QENS results were averaged into 30-min slices with data being taken continuously.

The QENS measurements were performed using the NIST Fermi chopper time-of-flight (TOF) spectrometer, which has an elastic scattering resolution of 0.146 meV [10]. Results were averaged over a  $|\vec{Q}|$  range from 1.9 to 2.4 Å<sup>−1</sup>, where  $\vec{Q}$ , the neutron scattering vector, is defined in terms of the change in neutron momentum upon scattering.

Due to hydrogen's extremely large incoherent scattering cross section, it tends to dominate the quasi-elastic neutron spectrum in hydrogenous materials. Thus, in the case of cement hydration, the results reflect the state of the water. The shape of the quasi-elastic spectra lead us to model the data using three separate components. The first was a Lorentzian peak of fixed width arising from free (liquid) water; the second was a Lorentzian peak of variable width arising from liquid water that was geometrically constrained by the cement gel; and the third was a Gaussian peak arising from water that had chemically reacted to form a solid product. A more complete explanation of this analysis technique is provided in Ref. [3] and leads to a final expression for the quasi-elastic scattering (Eq. (2)):

$$S_{inc}(Q, \omega) = C_0 + \left\{ A[\delta(\omega = 0)] + B_1 \left[ \frac{\Gamma_0}{\pi(\Gamma_0^2 + \omega^2)} \right] + B_2 \left[ \frac{\Gamma_2}{\pi(\Gamma_2^2 + \omega^2)} \right] \right\} \otimes \left( \frac{1}{\sigma\sqrt{2\pi}} e^{-1/2(\frac{\omega}{\sigma})^2} \right) \quad (2)$$

where  $C_0$  is a fixed baseline intensity,  $A$  is the number density of bound hydrogen atoms,  $B_1$  is the number density of free hydrogen atoms (all of which are assumed to be in the form of water),  $\Gamma_0$  is the Lorentzian full width at half maximum for bulk water,  $B_2$  is the number density of hydrogen atoms in the form of constrained water,  $\Gamma_2$  is a variable width fitting parameter and  $\sigma$  is the Gaussian

<sup>1</sup> Cement-chemistry notation: C=CaO, S=SiO<sub>2</sub>, H=H<sub>2</sub>O.

<sup>2</sup> Manufacturers are identified in order to provide complete identification of experimental conditions, and such identification is not intended as a recommendation or endorsement by the NIST.

<sup>3</sup> Powder obtained by courtesy of J. Francis Young, University of Illinois at Urbana Champaign.

standard deviation of the measured resolution of the spectrometer. From this, it is a simple matter to define both a FWI and a bound water index (BWI) given by (Eq. (3)):

$$\text{FWI} = \frac{B_1}{A + B_1 + B_2}$$

$$\text{BWI} = 1 - \text{FWI} = \frac{A + B_2}{A + B_1 + B_2} \quad (3)$$

The FWI represents the fraction of the initial water mixed with the cement that remains as bulk-like water, while the converse BWI represents the initial water fraction that is no longer bulk-like water.

#### 4. Results

Fig. 1 shows the time evolution of the BWI for two different  $\text{C}_3\text{S}$  pastes and an OPC paste cured at 20, 30 and 40 °C. Each type of paste exhibits the characteristic induction period, which is followed by a rapid rise in the reaction rate, and then finally a much slower reaction rate at later hydration times. The temperature dependence of the data for the first  $\text{C}_3\text{S}$  material is different from the other two in that it shows a crossing of the different temperature BWI curves. This cross-over phenomenon has been observed using other techniques and is thought to occur because the

nature of the C–S–H product formed varies with temperature [5,6]. The rate of hydration during the nucleation and growth period is always higher at higher temperature, but any variation in the C–S–H product morphology can greatly affect the subsequent diffusion limited kinetics and can lead to a behavior in which the hydration rate has an inverse temperature dependence. Whether this slower kinetics leads to a crossing in the BWI curves depends upon the level of hydration at which the reaction kinetics change from being growth limited to diffusion limited. As discussed in Ref. [3], this hydration level is determined by many factors, of which the most important appears to be the average particle size of the  $\text{C}_3\text{S}$  grains.

#### 5. Diffusion limited behavior

As the available pore space becomes filled with gel product further hydration occurs through growth inward into the  $\text{C}_3\text{S}$  grain and at some time the reaction becomes limited by the rate at which water can diffuse through the C–S–H surface layer to reach the unreacted  $\text{C}_3\text{S}$ . Fuji and Kondo [11] proposed a differential equation for the decrease of the radius  $r$  of the unreacted grain of the form (Eq. (4)):

$$-dr/dt = D^*/(R_d - r) \quad (4)$$

where  $D^*$  is an effective diffusion constant and  $R_d$  is the radius at time  $t_d$ , the onset of diffusion-controlled kinetics. If the number of water molecules reacting with each  $\text{C}_3\text{S}$  molecule remains relatively constant throughout the diffusion limited period, then it has been shown that the FWI has the form [1]:

$$(\text{FWI})^{1/3} = (\text{FWI}_d)^{1/3} - R^{-1}(2D^*)^{1/2}(t - t_d)^{1/2} \quad (5)$$

where  $\text{FWI}_d$  is the FWI of the system at time  $t_d$  and  $R$  is the original radius of the  $\text{C}_3\text{S}$  grain.

Fig. 2 shows the long time hydration data for all three systems plotted in terms of Eq. (5). The curves have been displaced for clarity, but in each case the data shows a linear dependence consistent with diffusion limited behavior at later hydration times. The extracted hydration rates (slope of the lines) are listed in Table 1. The results for the two  $\text{C}_3\text{S}$  systems are very similar, while the OPC samples show a somewhat larger rate. However, in all three systems, there is relatively little change in the diffusion rate with temperature. Diffusion is a thermally activated process that generally follows an Arrhenius behavior. As such one would expect a significant enhancement of the diffusion process with increasing temperature. A possible explanation for the observed temperature dependence of the measured diffusion rate is that at higher temperatures the nucleation and growth process forms a denser C–S–H layer around the  $\text{C}_3\text{S}$  grain. The increase in the intrinsic diffusion rate with temperature is thus offset by the formation of a more impervious

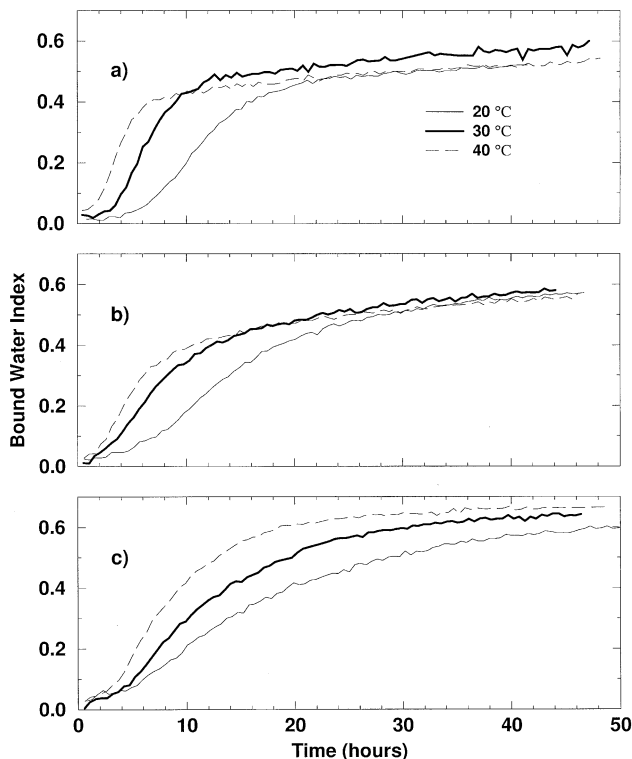


Fig. 1. Bound water index versus time for isothermal hydration at 20, 30 and 40 °C. (a)  $\text{C}_3\text{S}$  #1, (b)  $\text{C}_3\text{S}$  Batch #2, (c) Portland cement.

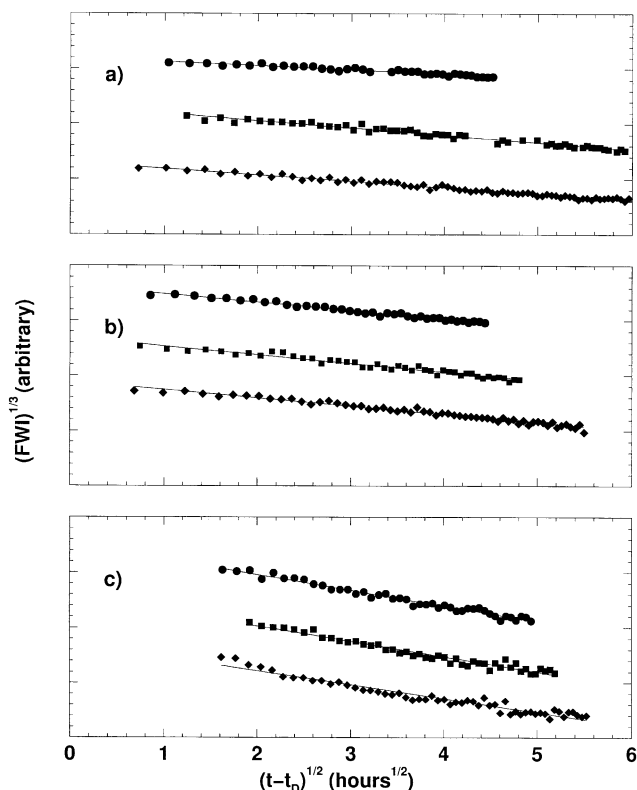


Fig. 2. Free water index at later hydration times fit to a diffusion limited behavior. Circles 40 °C, squares 30 °C, triangles 20 °C. The values for  $t_d$  are taken from Ref. [1]. The traces have been offset vertically for clarity. (a) C<sub>3</sub>S #1, (b) C<sub>3</sub>S Batch #2, (c) Portland cement.

medium through which diffusion must occur. These two factors appear to combine to produce a net effect that is largely temperature insensitive. This behavior is consistent with literature values which quote relatively small activation energies on the order of a few kJ/mol for diffusion limited

Table 1  
Diffusion rates for curing cement samples

Sample	Temperature, °C	Diffusion rate $\times 10^3$ ( $\text{h}^{-1/2}$ )
C <sub>3</sub> S Sample #1	20	$8.4 \pm 0.4$
	30	$11.8 \pm 0.3$
	40	$11.4 \pm 0.2$
C <sub>3</sub> S Sample #2	20	$15.2 \pm 0.4$
	30	$15.6 \pm 0.5$
	40	$14.9 \pm 0.3$
Portland cement	20	$28.4 \pm 0.7$
	30	$28.0 \pm 0.9$
	40	$25.4 \pm 0.9$
C <sub>3</sub> S Sample #1 Initially cured at 20 °C	20	$8.4 \pm 0.4$
	40	$16.7 \pm 0.3$
	80	$56.3 \pm 0.5$
C <sub>3</sub> S Sample #1 Initially cured at 40 °C	20	$2.5 \pm 0.3$
	40	$11.8 \pm 0.3$
	80	$36.6 \pm 0.4$

The values are determined by the slope of the curves shown in Figs. 2 and 3. For the 80 °C samples, the rates are those for the first 3 h immediately after the temperature increase at 24-h hydration.

hydration in C<sub>3</sub>S leading to a 10–15% increase in the diffusion constant between 20 and 40 °C [11,12].

To confirm this hypothesis and obtain a true value for the intrinsic activation energy, we performed a series of measurements in which the sample was cured at an initial temperature for approximately 24 h. The curing temperature was then changed and the hydration (which is now in the diffusion limited regime) was monitored at the second temperature. The results for the second stage of the experiment are shown in Fig. 3. The diffusion limited behavior in these C<sub>3</sub>S samples is again confirmed by the linearity of the curves. The middle two traces show the data for samples that were both monitored at 40 °C in the second stage. In the case of the open circles, the sample was initially cured at 40 °C, while the closed circles shows the data for samples initially cured at 20 °C. The marked difference in the slopes of the data obtained at the same temperature is quite dramatic. The fact that the sample initially cured at 20 °C has a significantly higher diffusion constant confirms that the initial C–S–H material formed at 20 °C is much more permeable to diffusion than that formed at the 40 °C. Similarly, the bottom two curves for samples monitored at 20 °C during the second stage also show quite different slopes. As expected, the paste initially cured at 40 °C and monitored at 20 °C shows the smallest diffusion rate of all the specimens measured.

The top two traces in Fig. 3 show the results for samples monitored at 80 °C during the second stage. These samples

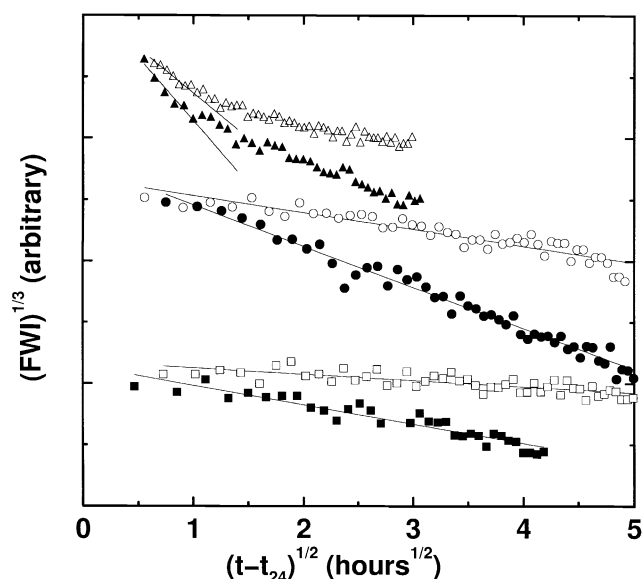


Fig. 3. Free water index fit to a diffusion limited behavior for times greater than 24 h. The traces have been offset vertically to show more clearly the differences in slopes for samples monitored at the same temperature. Upper traces: open triangles cured at 40 °C for 24 h and monitored at 80 °C; closed triangles cured at 20 °C for 24 h and monitored at 80 °C. Middle traces: open circles cured at 40 °C for 24 h and monitored at 40 °C; closed circles cured at 20 °C for 24 h and monitored at 40 °C. Lower traces: open squares cured at 40 °C for 24 h and monitored at 20 °C; closed squares cured at 20 °C for 24 h and monitored at 20 °C.

had been initially cured for 24 h at 20 and 40 °C, respectively. The analysis in this case proved more complicated. Although the slope of the data obtained for the first few hours after the temperature jump did show linear diffusion like behavior, the subsequent data points deviated significantly from this initial slope. We attribute this to the rapid formation of dense, impermeable product material at 80 °C. The initial slope to the FWI curve after the temperature jump represents diffusion through material that was predominantly formed at 20 (or 40 °C). However, after a few hours, the measured rate represents the diffusion through a layer that contains significant amounts of product formed at 80 °C, causing the deviation in slope.

Using the results for samples initially cured at 20 °C and monitored at 20, 40 and 80 °C, we were able to estimate that the activation energy for the diffusion process is on the order of 50 kJ/mol. The activation energy for the sample initially cured at 40 °C is roughly 40% larger than that of the 20 °C cured sample. These values are considerably higher than those previously quoted [11,12] since they now represent the intrinsic activation energy.

From the data in Table 1 and the fact that the initial radius  $R$  of the  $C_3S$  particles is approximately 7  $\mu\text{m}$ , Eq. (5) yields values for  $D^*$  on the order of  $10^{-15} \text{ cm}^2/\text{s}$ . These results are consistent with those of Fujii and Kondo [11] but should not be interpreted as the self diffusion constant for the unreacted water which (determined from the width of the quasi-elastic peak) is on the order of  $10^{-5} \text{ cm}^2/\text{s}$ . One would expect the effective diffusion constant controlling the reaction rate to be considerably smaller than the self-diffusion of water. However, the fact that they differ by some ten orders of magnitude suggests that although the model of Fujii and Kondo provides a very good estimate of the power law kinetics and an excellent method of comparing temperature dependence it is still oversimplified. A more complete model would include diffusion with reaction [13] or diffusion in an undersaturated pore system [14].

## 6. Conclusion

QENS is sensitive to the state of water in curing cementitious samples, and thus can be used to monitor the rate of conversion of liquid water to bound water. Hydration experiments conducted using two-stage temperature profiles showed that the rate of hydration at a given temperature during the later diffusion state was inversely dependent on the initial curing temperature. In some cases,

the degree of hydration at a higher curing temperature was actually less than that at lower temperatures. These results support the hypothesis that a more impermeable product layer is formed around the hydrating cement or  $C_3S$  grains when a higher temperature is used during the initial curing. In addition, it was found that the intrinsic activation energy for this diffusion process is much greater than the traditional values obtained using samples initially cured at different temperatures.

## Acknowledgments

This research has been partially supported by the ACS Petroleum Research Fund grant # 35452-GB5.

## References

- [1] S.A. FitzGerald, D.A. Neumann, J.J. Rush, D. Bentz, R.A. Livingston, In situ quasi-elastic neutron scattering study of the hydration of tricalcium silicate, *Chem. Mater.* 10 (1998) 397–402.
- [2] S.A. FitzGerald, D.A. Neumann, J.J. Rush, R.A. Livingston, R.J. Kirkpatrick, X. Cong, Inelastic neutron scattering study of the hydration of tricalcium silicate, *J. Mater. Res.* 14 (1999) 1160–1165.
- [3] J.J. Thomas, S.A. FitzGerald, D.A. Neumann, R.A. Livingston, The state of water in hydrating tricalcium silicate and Portland cement pastes as measured by quasi-elastic scattering, *J. Am. Ceram. Soc.* 84 (2001) 1811–1816.
- [4] E.J. Prosen, P.W. Brown, G. Frohnsdorff, F. Davis, A multichambered microcalorimeter for the investigation of cement hydration, *Cem. Concr. Res.* 15 (1985) 703–710.
- [5] S. Brunauer, D.L. Kantro, in: H.F.W. Taylor (Ed.), *The Chemistry of Cements*, vol. 1, Academic Press, New York, 1964, pp. 287–309.
- [6] A. Bentur, R.L. Berger, J.H. Kung, N.B. Milestone, J.F. Young, Structural properties of calcium silicate pastes: II. Effect of curing temperature, *J. Am. Ceram. Soc.* 62 (1979) 362–366.
- [7] M. Tarrida, M. Madon, B.L. Rolland, P. Colombet, An in-situ Raman-spectroscopy study of the hydration of tricalcium silicate, *Adv. Cem. Based Mat.* 2 (1995) 15–20.
- [8] H.F.W. Taylor, P. Barret, P.W. Brown, D.D. Double, G. Frohnsdorff, V. Johansen, The hydration of tricalcium silicate, *Mater. Constr.* 17 (1985) 457–468.
- [9] E.M. Gartner, J.M. Gaidis, in: J.P. Skalny (Ed.), *Materials Science of Concrete*, American Ceramic Society, Westerville, OH, 1989, p. 95.
- [10] J.R.D. Copley, T.J. Udovic, Neutron time-of-flight spectroscopy, *J. Res. Natl. Inst. Stand. Technol.* 98 (1993) 71–87.
- [11] K. Fujii, W. Kondo, Kinetics of the hydration of tricalcium silicate, *J. Am. Ceram. Soc.* 57 (1974) 492–497.
- [12] P.W. Brown, J. Pommersheim, G. Frohnsdorff, A kinetic model for the hydration of tricalcium silicate, *Cem. Concr. Res.* 15 (1985) 35–41.
- [13] E.L. Cussler, *Diffusion: Mass Transfer in Fluid Systems*, Cambridge Univ. Press, Cambridge, 1984.
- [14] C. Hall, Barrier performance of concrete—a review of fluid transport theory, *Mater. Struct.* 27 (1994) 291–306.